9. Supplementary Material

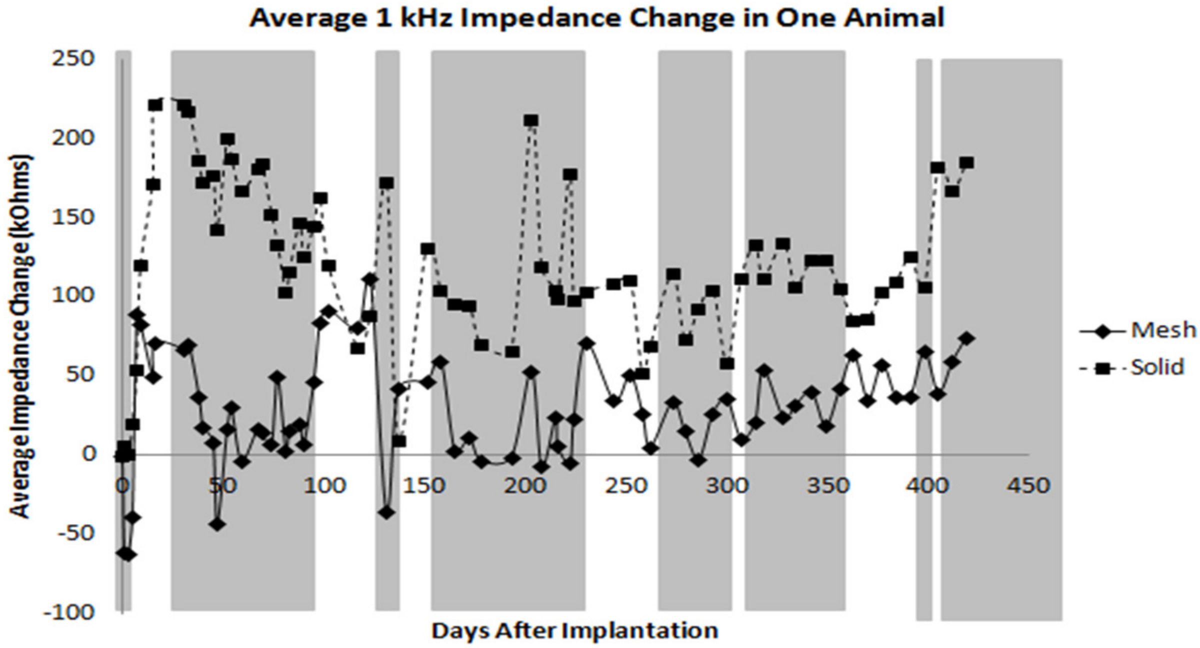

Supplemental Figure 1: Average longitudinal 1 kHz impedance data for mesh and solid micro-ECoG devices implanted in a single animal for over one year. Shaded regions represent time periods where there was a statistically significant difference in the mesh and solid impedance values ($p < 0.05$, student's t test). This data suggests that perhaps major differences in the mesh and solid impedance values may not be noticeable until greater than one month after implantation. Change in impedance was calculated from the first impedance measurement after implantation and averaged over all 16 channels on each device. If channels had 1 kHz impedance values greater than 1000 kOhms they were considered to be dead channels, and thus not included in the average.

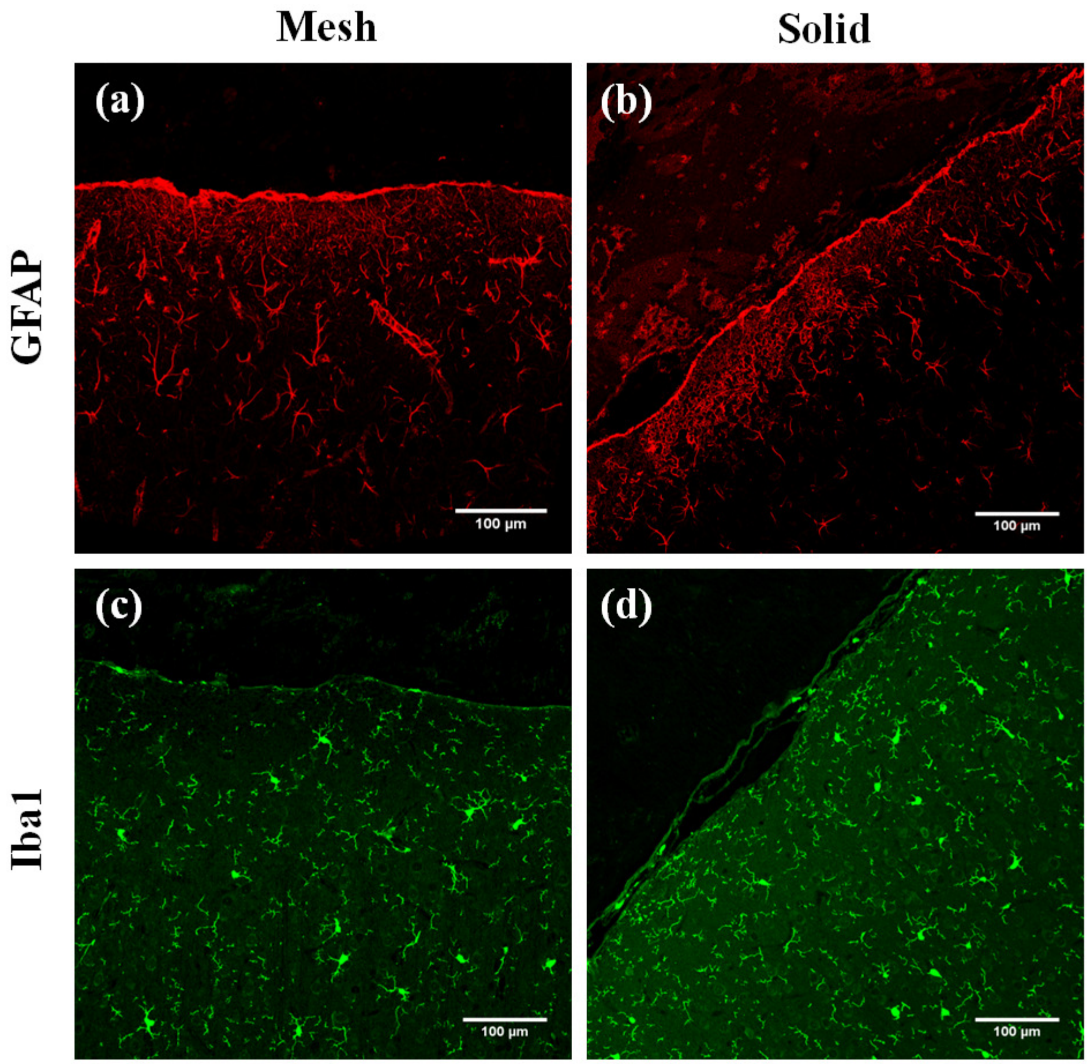

Supplemental Figure 2: Astrocyte and Microglia staining of cortical brain tissue sections below mesh and solid devices. **(a)** GFAP antibody staining of astrocytes in brain tissue below mesh device. **(b)** GFAP staining of astrocytes in brain tissue below solid micro-ECoG device. **(c)** and **(d)** Iba1 antibody staining of microglia in brain tissue below mesh and solid devices, respectively.

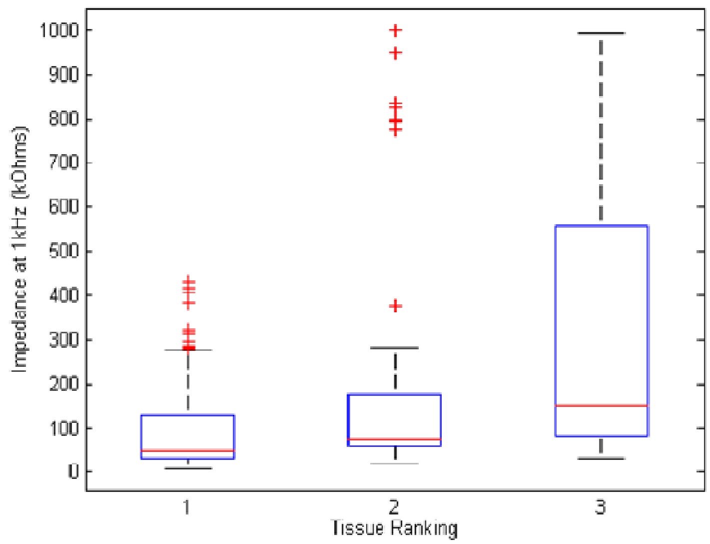

Supplemental Figure 3: The correlation between the amount of tissue around an electrode site and its 1 kHz impedance. One animal, which was implanted for one year and had variable tissue growth around different electrode sites was analyzed. One representative image was selected from each imaging session over the entire implantation period. Images were randomized and given to an individual who would rank each electrode site with a value of 1, 2 or 3. Tissue rankings were defined by the following criteria: 1: No visible scar tissue around the electrode site. 2: Some scar tissue visible around the electrode site, but site is still clearly visible through the cranial window. 3: Electrode site completely obscured by scar tissue.

Estimating refractive index using OCT

OCT Specifications

The customized SD-OCT device that was used in this paper uses an 8mW light source with spectral bandwidth of 200nm at the central wavelength of 1300nm. The interference patterns are captured by a 1024 pixel line-scan InGaAs camera capable of recording up to 91,900 axial scans per second. A 10x scan lens is used as the OCT objective with depth of focus of 160 μm. The zero path difference was set to 200 μm above the focal plane of the scan lens to take advantage of the whole depth of focus. The designed SD-OCT system provides transverse and axial resolution of 4μm and 5μm in free space, respectively.

Refractive Index Measurement

We estimated the refractive index of a sample by calculating the ratio of its optical to physical thickness. Both of these were obtained by processing the OCT image, similar to the method presented in ref (33). The optical thickness of the specimen was calculated directly from the OCT image, while its physical thickness was assessed by detecting the increment introduced by the sample to the optical path length and cancelling it out from the optical thickness. As shown in Supplemental Figure 5, the increase in the optical path length (*D*) can be calculated by measuring the displacement observed in the OCT image of a flat surface beneath the sample. Therefore, if we denote the physical and optical thicknesses with L and L_O respectively, then refractive index can be calculated by:

$$n = \frac{L_O}{L} = \frac{L_O}{L_O - D} \quad (1)$$

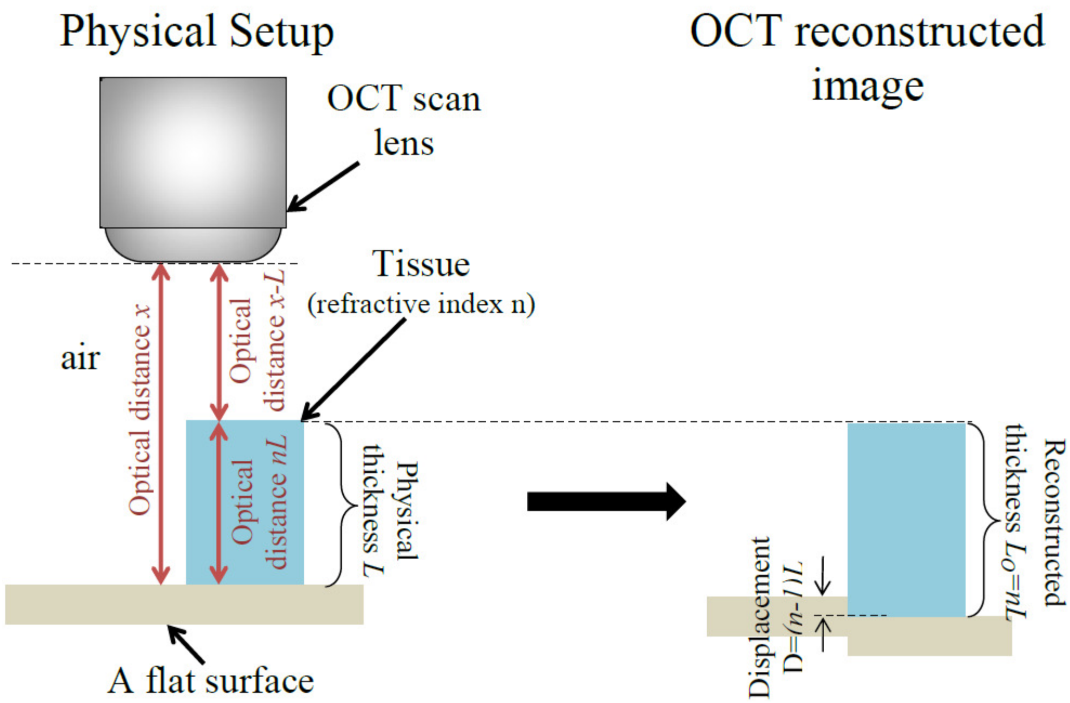

Supplemental Figure 4: The effect of change in the optical path in the reconstructed image.

Supplemental Figure 6(a) demonstrates an example of how refractive index was estimated using OCT scan of scar tissue. In this example, the displacement is D = 687−547 = 140 µm, and the thickness of the tissue is L_O = 656-219= 437 µm, which results in refractive index of $n = \frac{437}{437-140} = 1.47$.

By using this method, refractive indices of 15 samples were estimated and the results are shown in Supplemental Figure 6(b). The averaged refractive index was 1.39, while the standard deviation of the data was 0.0062, after removing the two outliers.

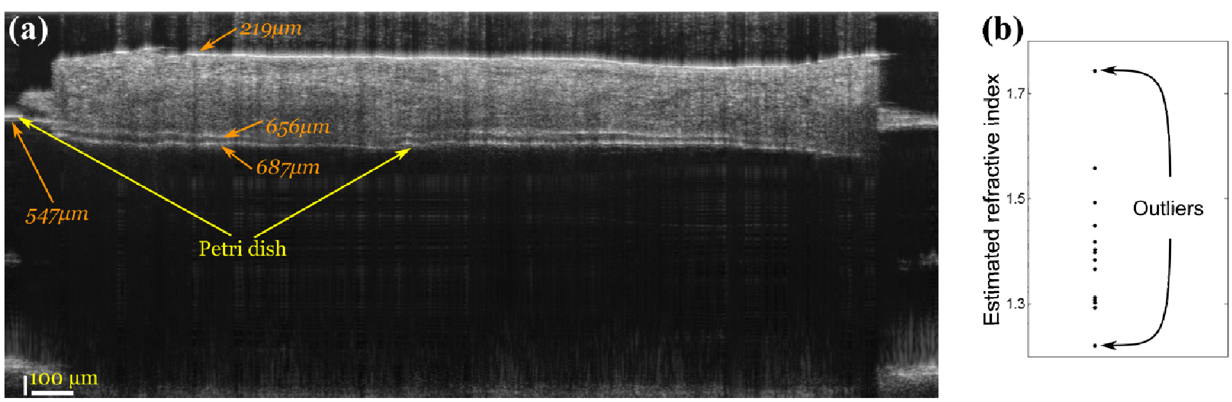

Supplemental Figure 5: Measurement of refractive index of scar tissue using SD-OCT. **(a)** an example data that was used to estimate the refractive index. Numbers in italic font specify the axial positions of corresponding points. **(b)** result of refractive index measurements for 15 samples in a petri dish.